일반논문 (Regular Paper)
방송공학회논문지 제30권 제6호, 2025년 11월 (JBE Vol.30, No.6, November 2025)
https://doi.org/10.5909/JBE.2025.30.6.1072
ISSN 2287-9137 (Online) ISSN 1226-7953 (Print)

ATSC 3.0 시스템에서 DFT 기반 채널 추정을 위한 적응형 Windowing 기법

고 영 빈[a], 김 정 창[a)‡]

Adaptive Windowing Scheme for DFT-Based Channel Estimation in ATSC 3.0 System

Youngbin Go[a)] and Jeongchang Kim[a)‡]

요 약

DFT (discrete Forurier fransform) 기반 채널 추정은 낮은 계산 복잡도와 우수한 성능 때문에 파일럿 기반 시스템에서 널리 사용되고 있다. DFT 기반 채널 추정은 채널 임펄스 응답 (channel impulse response: CIR)에서 windowing을 통해 잡음의 영향을 줄임으로써 성능을 향상시킨다. 기존 DFT 기반 채널 추정은 windowing을 위해 고정된 파라미터를 사용한다. 그러나, 채널 환경은 바뀔 수 있기 때문에, 고정된 파라미터는 채널 추정 성능 저하를 야기할 수 있다. 그러므로, 채널 환경의 변화에 대응하기 위해 적응형 windowing 기법이 필요하다. 본 논문에서는 채널 변화에 따라 윈도우 크기를 적응적으로 조절할 수 있는 DFT 기반 채널 추정을 위한 적응형 windowing 기법을 제안한다. 전산 실험은 한국에서 방송 시스템 표준으로 채택된 ATSC (Advanced Television Systems Committee) 3.0 표준 기반의 다양한 채널 환경에서 수행되었고, 전산 실험 결과를 통해 제안하는 기법이 기존 기법보다 성능이 우수함을 확인할 수 있다.

Abstract

The discrete Fourier transform (DFT)-based channel estimation is widely used in pilot-aided systems, due to its low complexity and good performance. It enhances performance by reducing the impact of noise through windowing in the channel impulse response (CIR). The conventional DFT-based channel estimation uses fixed parameters for windowing. However, since the channel environment can be varied, fixed parameters may lead to degradation in channel estimation performance. Therefore, an adaptive windowing scheme is needed to accommodate variations in channel conditions. In this paper, we propose an adaptive windowing scheme for DFT-based channel estimation that can adaptively adjust the window size to channel variations. Simulations are performed under various channel environments based on Advanced Television Systems Committee (ATSC) 3.0 standard adopted in Korean broadcasting system, and the results show that the proposed scheme outperforms the conventional schemes.

Keyword : Adaptive windowing, ATSC 3.0, Channel estimation, DFT, Scattered pilot

Ⅰ. Introduction

In wireless communications, transmitted signals are distorted by fading due to channel effects such as path loss, reflection, refraction, and delay spread in multipath channels[1]. Signal distortion due to fading makes demodulation difficult, which leads to performance degradation. Therefore, accurate channel estimation is crucial for achieving optimal performance. Channel estimation can be conducted through blind channel estimation, which utilizes the statistical characteristics of the transmitted signal, or pilot-based channel estimation[2][3]. Recently, many wireless communication systems have been designed based on orthogonal frequency division multiplexing (OFDM), and channel estimation has been performed using pilot symbols.

Most wireless communication systems, including fifth-generation new radio (5G NR) and Advanced Television Systems Committee (ATSC) 3.0, employ scattered pilots for channel estimation[4][5]. Scattered pilots are inserted in regular patterns in the time-frequency domain, enabling least square (LS)-based channel estimation[6]. The LS is performed to calculate the channel gain through transmitted and received pilot symbols. LS-based channel estimation is straightforward to implement. While LS estimation is computationally efficient, it is susceptible to errors caused by additive background noise. To reduce the channel estimation errors, minimum mean squared error (MMSE) channel estimation is commonly used[7]. The MMSE channel estimation utilizes statistical characteristics, such as the covariance of channel gains and the covariance of noise, to mitigate channel estimation errors.

a) 국립한국해양대학교 전자통신공학과 해양인공지능융합전공(Interdisciplinary Major of Maritime AI Covergence, Department of Electronics and Communications Engineering, Korea Maritime & Ocean University)
‡ Corresponding Author : 김정창(Jeongchang Kim)
E-mail: jchkim@kmou.ac.kr
Tel: +82-51-410-4315
ORCID: https://orcid.org/0000-0002-8612-9360
· Manuscript September 24, 2025; Revised October 27, 2025; Accepted October 27, 2025.

After estimating the channel gains corresponding to pilot symbols using the least square and MMSE channel estimations, the channel gain of data symbols can be obtained by interpolating the channel gains of the scattered pilots. The channel frequency response (CFR) can then be obtained from the channel gains of both pilot and data symbols. Linear interpolation is a well-known method with very low computational complexity, but it suffers from significant performance degradation[8].

Discrete Fourier transform (DFT)-based channel estimation can be used to reduce channel estimation errors[9]. Using the channel gains of pilot symbols, a channel impulse response (CIR) can be obtained through inverse discrete Fourier transform (IDFT). Then, unwanted components in the CIR caused by noise are suppressed with a windowing filter, and the filtered CIR is transformed into the CFR through DFT operation. The performance of the DFT-based channel estimation depends on how effectively unwanted components in the CIR are filtered, and many studies have been conducted to improve performance[10-18]. However, in previous studies, filtering was performed using fixed values of design parameters, such as window size and threshold, leading to performance deterioration when the channel environment varied. Therefore, adaptive filtering is required to cope with various channel conditions.

In this paper, we propose an adaptive windowing scheme for DFT-based channel estimation in scattered pilot systems. In the proposed scheme, a given number of samples with the longest delays in the CIR are considered unwanted components caused by noise. The power of the undesirable components in the CIR is calculated and subtracted from the total power of the CIR. The remaining power can then be considered a multipath component, and windowing is performed based on the ratio of multipath components in the total CIR. Therefore, the window size is set adaptively depending on the channel condition.

The simulations are performed to evaluate the performance of the proposed scheme. In this paper, the Rayleigh

20-path (RL20) and the Typical Urban 6-path (TU-6) channels are considered as fixed and mobile reception environments[22][23]. These channel models have been widely employed in studies that measured and analyzed reception performance in the ATSC 3.0-based Korean broadcasting system[27][28]. In addition, a single frequency network (SFN) channel model built on measurements obtained from the operating network in the Seoul Metropolitan area is also considered[29].

This paper consists of the following sections. In section 2, the system model of the received signal is briefly described. Section 3 introduces conventional DFT-based channel estimation schemes, and the proposed windowing scheme for DFT-based channel estimation is described in section 4. In section 5, simulation results compare the performance of the conventional and proposed schemes under varying channel conditions. Finally, this paper is concluded in section 6.

Ⅱ. System Model

In this section, the frame structure of a scattered pilot system and the received signal model are described. In this paper, the frame structure of the ATSC 3.0 standard is assumed as a scattered pilot system[24-26].

1. Frame Structure of ATSC 3.0

The physical layer frame of ATSC 3.0 includes various pilots, such as preamble pilot, edge pilot, subframe boundary pilot, common continuous pilot, additional continuous pilot, and scattered pilot (SP). They are inserted into the frame according to the given rules and serve the purpose of channel estimation. Fig. 1 shows an example of the frame structure of ATSC 3.0 with pilots. Especially, the SPs are distributed across the time-frequency domain of the frame in a regular pattern. The configuration of SPs varies

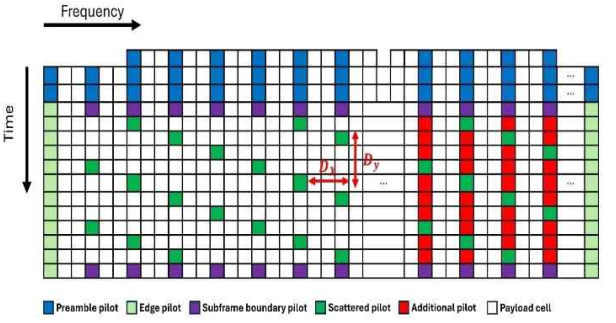

그림 1. 파일럿이 포함된 ATSC 3.0 프레임 구조
Fig. 1. Frame Structure of ATSC 3.0 with pilots

depending on the guard interval (GI) and fast Fourier transform (FFT) size and are denoted as $\mathrm{SP}D_x\_D_y$. Here, D_x and D_y represent the number of subcarriers between adjacent SPs in the frequency domain and the number of OFDM symbols forming one SP sequence, respectively. Channel estimation is performed by obtaining the channel gains of SPs and interpolating them to derive the channel gains of data symbols. However, the channel gains of data subcarriers at the edges of the time or frequency domain cannot be obtained solely through the interpolation of scattered pilots. To address this problem, the edge pilot and subframe boundary pilot are inserted to perform frequency and time interpolation at the edges.

2. Signal Model of Received Signal

The frequency domain data $X_l(k)$ is transformed into a time domain transmission signal through the inverse fast Fourier transform (IFFT) where l and k denote the OFDM symbol and the subcarrier indices, respectively. The transmission signal is represented as

$$x_l(n) = \frac{1}{N}\sum_{k=0}^{N-1} X_l(k) e^{j2\pi\frac{kn}{N}} \quad (1)$$

where $x_l(n)$ denotes the transmission signal for n-th OFDM sample of l-th OFDM symbol and N is the IFFT size. The transmitted signal passes through the channel and

is received. The received signal for n-th sample of l-th OFDM symbol, $y_l(n)$, is represented as

$$y_l(n) = h_l(n) \otimes x_l(n) + w_l(n) \tag{2}$$

where $h_l(n)$ and $w_l(n)$ denote the CIR in the time domain and additive white Gaussian noise (AWGN) for n-th sample of l-th OFDM symbol, respectively. The CIR refers to the response at the output when a unit impulse signal is applied to the channel and is represented as

$$h_l(n) = \sum_{i=1}^{L} a_{i,l}\delta[n - \tau_{i,l}] \tag{3}$$

where L, $a_{i,l}$, and $\tau_{i,l}$ denote the number of multipaths in the channel, the channel gain of each path, and the time delay of each path, respectively.

The received signal in the time domain is transformed into the frequency domain signal through the FFT. The received signal for k-th subcarrier of l-th OFDM symbol, $Y_l(k)$, is represented as

$$Y_l(k) = H_l(k)X_l(k) + W_l(k) \tag{4}$$

where $H_l(k)$, $X_l(k)$, and $W_l(k)$ denote CFR, transmitted signal, and AWGN for k-th subcarrier of l-th OFDM symbol, respectively.

Ⅲ. DFT-Based Channel Estimation

In this section, DFT-based channel estimation and its variated algorithms are described

1. DFT-Based Channel Estimation Algorithm

Fig. 2 shows the block diagram of DFT-based channel estimation. First, the least square is performed to obtain the channel gains of pilot subcarriers. The channel gains of the pilot subcarriers are obtained using transmitted and received pilots through the least square as follows

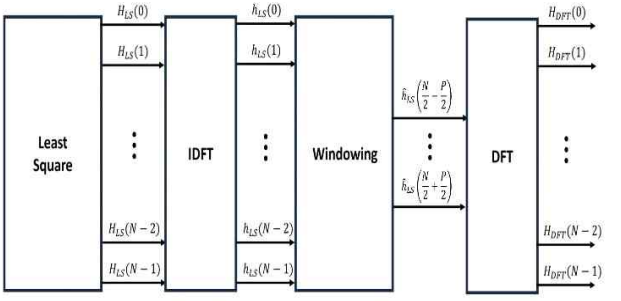

그림 2. DFT 기반 채널 추정의 블록 다이어그램
Fig. 2. Block diagram of DFT-based channel estimation

$$\hat{H}_{LS}(p) = arg \min_{H_{LS}(p)} |Y(p) - X(p)H_{LS}(p)|^2 \tag{5}$$

where $\hat{H}_{LS}(p)$ denotes the channel gain of p-th pilot subcarrier. Since it is applied identically to all OFDM symbols, we omit the OFDM symbol index in the following formula for simplicity. To find the $H_{LS}(p)$ that minimizes the equation $|Y(p) - X(p)H_{LS}(p)|^2$, the partial derivative of the equation $|Y(p) - X(p)H_{LS}(p)|^2$ is derived and represented as

$$\frac{\partial[(Y(p) - X(p)H_{LS}(p))^H(Y(p) - X(p)H_{LS}(p))]}{\partial H_{LS}(p)} = 0 \tag{6}$$

where the superscript H in the equation $(Y(p) - X(p)H_{LS}(p))^H$ denotes the Hermitian transpose. Then the solution of equation (6) is represented as

$$H_{LS}(p) = X(p)^{-1}Y(p) = H(p) + X(p)^{-1}W(p) \tag{7}$$

After obtaining channel gains for pilot subcarriers, zero-padding is performed for the channel gains of data

subcarriers, and then the IDFT is performed to obtain the CIR as follows

$$h_{LS}(n) = \frac{1}{N}\sum_{k=0}^{N-1} H_{LS}(k) e^{j\frac{2\pi}{N}nk} \tag{8}$$

where $h_{LS}(n)$ denotes the estimated CIR in the time domain.

The CIR represents the multipath profile of the channel. Since unwanted components can be induced by the noise, the channel estimation error can be reduced by rejecting unwanted components caused by the noise. To suppress unwanted components of the CIR, a windowing scheme can be applied. A straightforward windowing scheme is to eliminate the CIR components of the delay longer than the possible maximum delay of the channel. The maximum delay of the channel can be estimated by considering the multipath characteristics within the coverage area[19]. Also, the scattered pilots are positioned at regular intervals in the frequency domain, exhibiting periodicity. A signal with periodicity in the frequency domain appears repeatedly in the time domain due to the properties of the Fourier transform[20]. In ATSC 3.0 system, SPs are placed with a spacing of D_x in the time domain and D_y in the frequency domain. Therefore, the effective length of the CIR, P, can be represented as

$$P = \frac{N}{D_x D_y} \tag{9}$$

Then, by taking the CIR of length P, the unwanted components caused by the noise can be eliminated, and can be represented as

$$\hat{h}_{LS}(n) = \begin{cases} h_{LS}(n), & \frac{N}{2}-\frac{P}{2} \le n \le \frac{N}{2}+\frac{P}{2} \\ 0, & otherwise \end{cases} \tag{10}$$

After the windowing, the CIR is transformed to CFR through DFT and represented as

$$H_{DFT}(k) = \sum_{n=0}^{N-1} \hat{h}_{LS}(n)\, e^{-j\frac{2\pi}{N}kn} \tag{11}$$

Despite the windowing, since unwanted components caused by the noise may still exist, the channel estimation performance can be further improved by removing residual unwanted components within the window.

2. Conventional Post-Processing for DFT-Based Channel Estimation

Many studies have been conducted to eliminate unwanted components, and several schemes are introduced in this section. Fig. 3 shows the block diagram of conventional post-processing to eliminate residual unwanted components for DFT-based channel estimation.

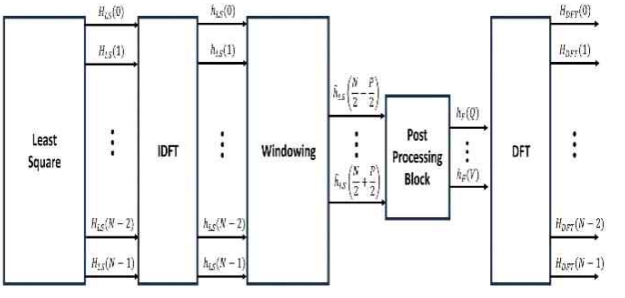

그림 3. 후처리 블록이 포함된 DFT 기반 채널 추정 블록 다이어그램
Fig. 3. Block diagram of DFT-based channel estimation with post-processing block

2.1 Fixed Size Window Scheme

Wireless communication systems are designed to ensure the CIR can accommodate the maximum delay of the channel. Then, the maximum delay is estimated by considering the multipath characteristics within the coverage area. Therefore, a fixed size window can be set considering the

maximum delay of the channel, allowing the elimination of unwanted components with delays longer than the window size[10-13]. The fixed size window scheme can be represented as

$$h_F(n) = \begin{cases} \hat{h}_{LS}(n), & Q \le n \le V \\ 0, & otherwise \end{cases} \quad (12)$$

where $h_F(n)$ denotes CIR after post-processing. Also, Q and V denote the start and end indices of the window, respectively. Through the appropriate setting of a fixed-size window, unwanted components can be eliminated, improving channel estimation performance. However, as the actual multipath environment changes, there may be paths with longer delays than the set window. Paths with longer delays than the set window are ignored, which causes degradation in channel estimation performance.

2.2 Threshold Test Scheme

Using a fixed-size window, paths with longer delays than the window are ignored. Therefore, a threshold test can be employed to include the actual multipath components of the channel[14-16]. A sufficient signal-to-noise ratio (SNR) must be ensured for reliable wireless communication, and under a high SNR condition, the power of desired components of the channel response will be greater than the unwanted components caused by the noise. Therefore, a threshold test can be used to consider components with high power due to multipath and utilize them for channel estimation. The threshold test scheme can be represented as

$$h_F(n) = \begin{cases} \hat{h}_{LS}(n), & \left|\hat{h}_{LS}(n)\right| > Th \\ 0, & otherwise \end{cases} \quad (13)$$

where Th denotes the threshold value. This approach effectively filters out noise-induced components while retaining significant multipath components, thereby improving channel estimation accuracy. However, if the SNR is not sufficiently ensured, the power of the desired components may not be guaranteed and may be ignored. Also, if the threshold value is too small, more unwanted components may be included.

2.3 Maximum Points Selection Scheme

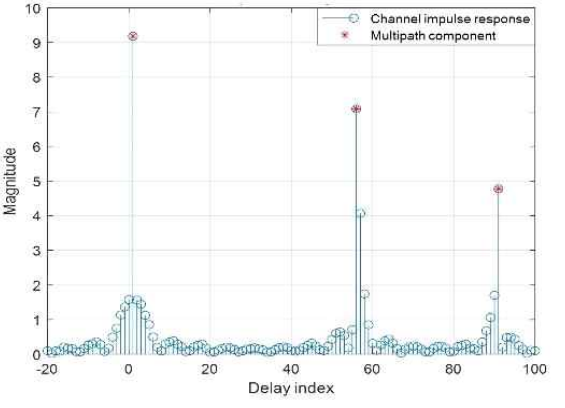

그림 4. Leakage effect의 예시
Fig. 4. Example of leakage effect

When a sufficiently high SNR is ensured, the power of desired components is greater than those caused by the noise. Therefore, channel estimation can be performed instead of a threshold test using only a given number of the largest components in the CIR[17]. This scheme, known as the maximum points selection scheme, involves sorting the CIR by magnitude and selecting only the pre-determined number of maximum points for channel estimation. Only multipath components can be utilized for channel estimation by appropriately setting the number of maximum points. However, some multipath components may be ignored if the number of maximum points is smaller than the number of multipaths.

In OFDM systems, zeros are padded at both ends of the bandwidth to prevent inter-channel interference (ICI), which is referred to as guard band (GB). The GB serves

to limit bandwidth, and a bandwidth-limited signal appears to be spread out after IDFT due to the properties of the Fourier transform. The spreading of bandwidth-limited signals after IDFT is called a leakage effect. Fig. 4 illustrates an example of the leakage effect[21]. In the maximum points selection scheme, the components are selected in descending order of magnitude, which may not include the dispersed components. To improve channel estimation performance, these dispersed components must also be incorporated into the channel estimation process.

2.4 Threshold-Based Window Size Setting Scheme

Windowing can be applied using a fixed window size to incorporate the dispersed components caused by the leakage effect in channel estimation. However, a fixed-size window may lead to performance degradation as the channel varies. Therefore, a scheme for adaptively adjusting the window size is needed to accommodate variations in the maximum delay of the channel.

To include the maximum delay of the channel, the window size can be set based on a threshold test[18]. First, a threshold test is performed on the CIR to identify components that exceed the threshold. Then, the earliest and latest paths among the components exceeding the threshold are identified and designated as the most advanced and most delayed paths of the channel, respectively. Finally, the window size is set based on the component designated as the most advanced and most delayed path, and windowing is performed. The threshold-based window size setting scheme can be represented in the same way as equation (12), where Q and V denote the indices of the most advanced and most delayed paths, respectively. Note that if the threshold is not set appropriately, multipath components may be ignored or excessive unwanted components may be included, potentially leading to degradation in channel estimation performance.

Ⅳ. Proposed DFT-Based Channel Estimation Scheme

In the previous section, conventional DFT-based channel estimation schemes were introduced. They utilize fixed parameters such as window size and threshold to eliminate unwanted CIR components. However, filtering with fixed parameters may ignore multipath components as the channel condition changes, degrading channel estimation performance. Therefore, an adaptive windowing scheme is necessary to accommodate changes in the multipath environment.

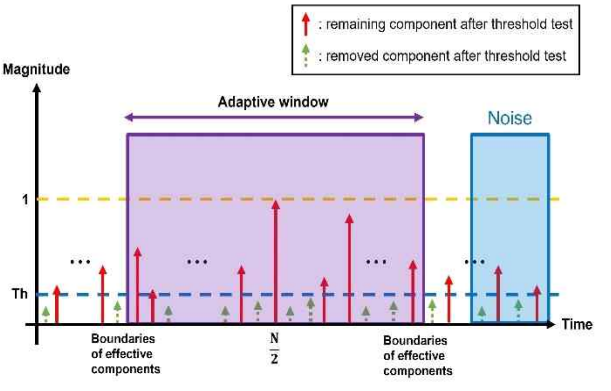

그림 5. 전력 측정 기반 적응형 윈도우 방식의 DFT 기반 채널 추정
Fig. 5. DFT-Based channel estimation with adaptive window based on power calculation

In this section, a power calculation-based adaptive windowing scheme is proposed. Fig. 5 shows an example of the adaptive windowing scheme based on power calculation. We assume that the CIR obtained from DFT is long enough to include the maximum delay of the channel. Then, a part of the samples located at the edge of the CIR can be considered as unwanted components caused by noise rather than multipath components. Therefore, the average power of these samples is calculated as the average power of the components caused by noise, which can be represented as

$$\sigma^2 = E\left[\left|\hat{h}_{LS}(n)\right|^2\right], \quad N-k \le n \le N \tag{14}$$

where σ^2 and k denote the average power of the unwanted components caused by noise and the number of samples used for calculating the average power of unwanted components. After calculating the average power of unwanted components, the average power of multipath components can be calculated by subtracting the average power of unwanted components from the average power of the CIR. If the average power of CIR is normalized to 1, the average power of the multipath components becomes $1-\sigma^2$. Using the average power of unwanted components, a threshold test is performed and can be represented as

$$h_{th}(n) = \begin{cases} \hat{h}_{LS}(n), & \left|\hat{h}_{LS}(n)\right| > \sigma \\ 0, & otherwise \end{cases} \tag{15}$$

where $h_{th}(n)$ denotes CIR after threshold test. Components smaller than the threshold can be considered unwanted and eliminated through a threshold test. Subsequently, the remaining components undergo windowing. The window size for this process can be determined based on the power of the multipath components. The proposed scheme accumulates the power from the components with shorter delays and identifies the index at which the total accumulated power equals the calculated average power of the multipath components. Then, the identified index is set as the boundary of the window, and the windowing is then performed based on this boundary. The proposed scheme determines the window size by calculating the power of unwanted components, enabling adaptive windowing even when the multipath environment changes.

Ⅴ. Simulation Results

In this section, the performance of conventional and proposed DFT-based channel estimations is provided. Computer simulations were conducted using TU-6, RL20, and Seoul SFN 1 channels to evaluate the performance of both conventional and proposed schemes under varying multipath environments[22][23][29]. The system parameters for computer simulations are described in Table 1.

표 1. 전산 실험을 위한 시스템 파라미터
Table 1. System Parameters for computer simulations

Parameter	Value
Center Frequency	500 MHz
System Bandwidth	6 MHz
Pilot Pattern	SP4_2
Modulation Order	16 QAM
FFT Size	8192
Channel Model	TU-6[22], RL20[23], Seoul SFN 1[29]

The simulations assume perfect synchronization between the transmitter and receiver. The center frequency was set to 500 MHz within the ultra-high frequency (UHF) band used for terrestrial broadcasting in South Korea. The system bandwidth is set to 6 MHz, the service bandwidth used in terrestrial broadcasting. The pilot pattern was set with $D_x = 4$ and $D_y = 2$. The FFT size is set to 8192, and the interval of scattered pilots in the frequency domain is 8. Therefore, the effective length of the CIR is 1024.

First, computer simulations are conducted on the TU-6 channel to determine the optimal parameters for conventional schemes. Fig. 6 shows the block error rate (BLER) performance according to the window size for the fixed size window scheme in the TU-6 channel. The maximum delay of the TU-6 channel is $5us$, corresponding to 35 samples

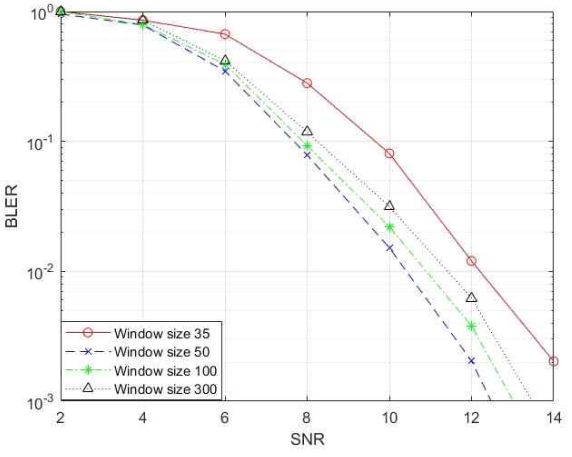

그림 6. TU-6 채널에서 고정 크기 윈도우 기법의 윈도우 크기에 따른 BLER 성능
Fig. 6. BLER performance according to the window size for the fixed size window scheme in TU-6 channel

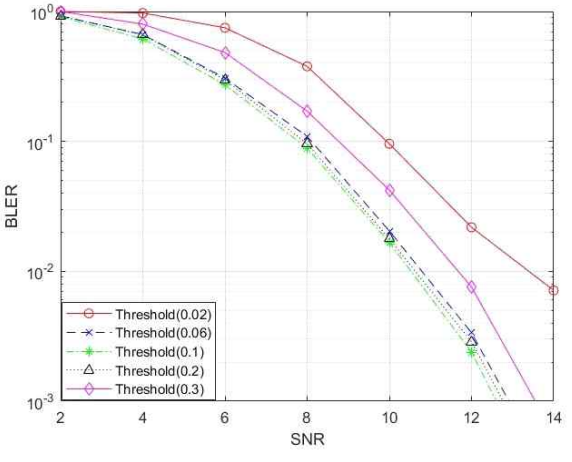

그림 7. TU-6 채널에서 임계값 기법의 임계값에 따른 BLER 성능
Fig. 7. BLER performance according to the threshold for the threshold test scheme in TU-6 channel

in the simulation. The BLER performance degrades as the window size increases, with a window size of 50 outperforming the maximum delay of 35. This is due to the leakage effect, which disperses the multipath components into surrounding paths. Therefore, a margin was added beyond the maximum delay, and a window size of 50 was set as the optimal parameter.

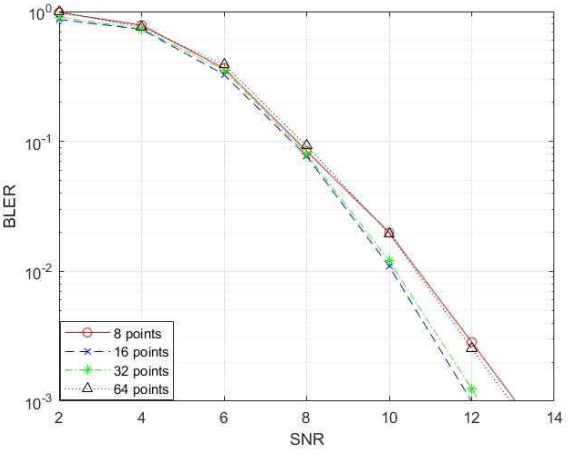

그림 8. TU-6 채널에서 최대점 선택 기법의 최대점 수에 따른 BLER 성능
Fig. 8. BLER performance according to the number of maximum points for the maximum points selection scheme in TU-6 channel

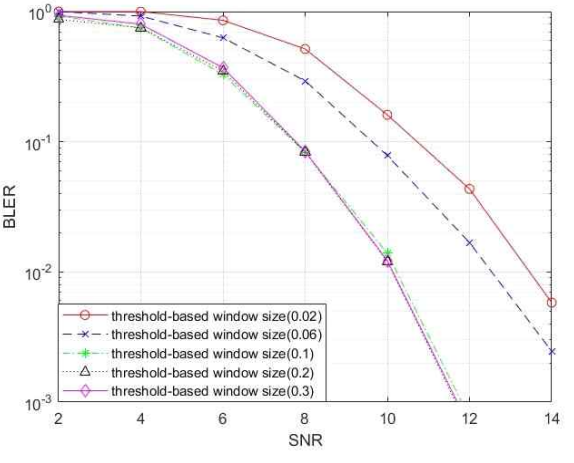

그림 9. TU-6 채널에서 임계값 기반 윈도우 크기 설정 기법의 임계값에 따른 BLER 성능
Fig. 9. BLER performance according to the threshold for threshold-based window size setting scheme in TU-6 channel

Fig. 7 shows the BLER performance according to a threshold for the threshold test scheme in the TU-6 channel. In Fig. 7, the threshold value of 0.1 shows the best performance. Higher threshold values lead to more multipath components being ignored, while lower valuesresult in the inclusion of more unwanted components,

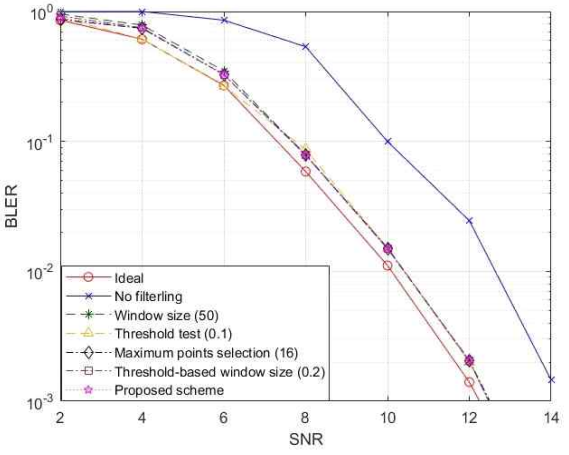

그림 10. TU-6 채널에서 DFT 기반 채널 추정 기법들의 BLER 성능
Fig. 10. BLER performance of DFT-based channel estimation schemes in TU-6 channel

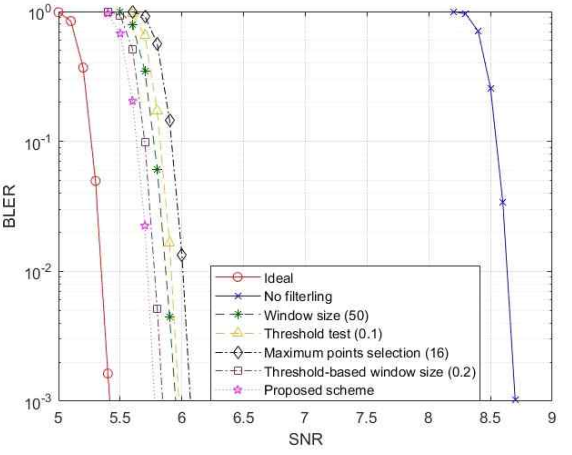

그림 11. RL20 채널에서 DFT 기반 채널 추정 기법들의 BLER 성능
Fig. 11. BLER performance of DFT-based channel estimations in RL20 channel

both resulting in performance degradation. Therefore, the threshold value of 0.1 was selected as the optimal threshold.

Fig. 8 shows the BLER performance according to the number of maximum points for the maximum points selection scheme in the TU-6 channel. In Fig. 8, selecting 16 maximum points shows the best performance. Increasing the number of maximum points leads to the inclusion of more unwanted components, while decreasing maximum points results in ignored multipath components, both resulting in performance degradation. Therefore, 16 was set as the optimal number of maximum points.

Fig. 9 shows the BLER performance according to threshold-based window size for the threshold test scheme in the TU-6 channel. In Fig. 9, a threshold value of 0.2 shows a slight performance gain over 0.1 and 0.3. Similar to the threshold test, extreme threshold values may result in performance degradation. Therefore, 0.2 was set as the optimal threshold value.

The optimal parameters of conventional schemes in the TU-6 channel are obtained through simulations. Fig. 10 shows the performance comparison of the DFT-based channel estimation schemes under the TU-6 channel. ‘Ideal’ represents the performance when all subcarriers within an OFDM symbol are used as pilots. The ‘No filtering’ represents windowing using the effective length of the CIR. The conventional schemes utilize pre-determined optimal parameters obtained through simulations. The ‘Proposed scheme’ represents the power calculation-based scheme that operates adaptively to channel variations. The ideal scheme shows the best performance, while no filtering shows the worst. The window size, threshold test, maximum points selection, threshold-based window size, and the proposed schemes show almost the same performance. This is because the conventional schemes use parameters optimized for the TU-6 channel, achieving the best performance.

To evaluate the performance of each scheme under varied multipath environments, the same pre-determined parameters are applied to the RL20 channel. Fig. 11 shows the performance comparison of various DFT-based channel estimation schemes under the RL20 channel. When the determined optimal parameters for the TU-6 channel are applied to the RL20 channel, the performance in order from

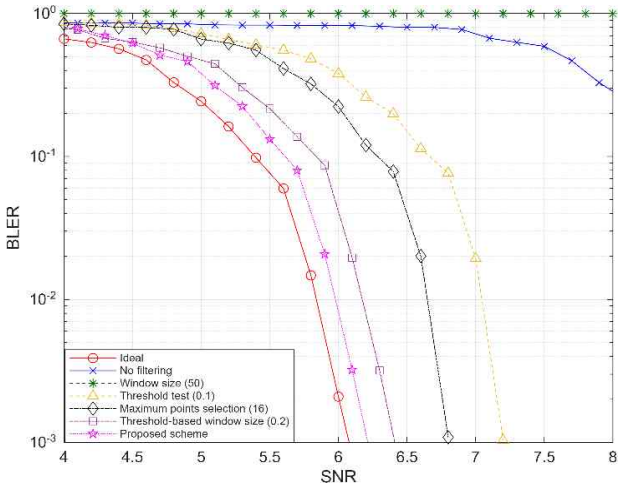

그림 12. Seoul SFN 1 채널에서 DFT 기반 채널 추정 기법들의 BLER 성능
Fig. 12. BLER performance of DFT-based channel estimations in Seoul SFN 1 channel

best to worst is ‘Ideal’, ‘Proposed scheme’, ‘Threshold-based window size’, ‘Window size’, ‘Threshold test’, ‘Maximum points selection’, and ‘No filtering’, from best to worst. This is because conventional schemes use fixed pre-determined parameter values regardless of the multipath environment. However, the proposed scheme adaptively performs windowing according to the channel environment, demonstrating superior performance in varying channel conditions.

In addition, the performance of each scheme was evaluated in the Seoul SFN 1 channel environment using the same pre-determined parameters. Fig. 12 shows the performance comparison of various DFT-based channel estimation schemes under the Seoul SFN 1 channel. When the determined optimal parameters for the TU-6 channel are applied to the Seoul SFN 1 channel, the performance in order from best to worst is ‘Ideal’, ‘Proposed scheme’, ‘Threshold-based window size’, ‘Maximum points selection’, ‘Threshold test’, and ‘No filtering’, from best to worst. The ‘window size’ could not demodulate the signal. This is because it was configured to accommodate the short delays of the TU-6 channel and therefore could not include the longer delays in the Seoul SFN 1 channel. As in the case of the RL20 channel, the conventional schemes use fixed, pre-determined parameter values regardless of the multipath environment. Therefore, the proposed method demonstrates superior performance because it performs windowing adaptively according to the channel conditions.

Ⅵ. Conclusion

In this paper, an adaptive windowing scheme for DFT-based channel estimation in scattered pilot was proposed. The proposed adaptive windowing scheme for DFT-based channel estimation can adaptively adjust the window size to channel variations. Simulations are performed under various channel environments based on the ATSC 3.0 standard adopted in the Korean broadcasting system. The simulation results show that the proposed scheme outperforms conventional schemes even in a multipath environment. Since conventional DFT-based channel estimation schemes use fixed pre-determined parameters regardless of the channel environment, the performance deteriorates when the channel condition varies. However, since the proposed scheme can adaptively adjust the window size according to the channel conditions, it can effectively adapt to channel variations.

참 고 문 헌 (References)

[1] K. M. Noga and B. Palczynska, “Overview of Fading Channel Model,” *Journal of Electronics and Telecommunications*, vol. 56, no. 4, pp. 339-344, Sep. 2010.
doi: https://dx.doi.org/10.2478/v10177-010-0044-x

[2] C. Tseng, Y. Cheng Cheng and C. Chung, “Subspace-Based Blind Channel Estimation for OFDM by Exploiting Cyclic Prefix,” *Journal of Wireless Communications*, vol. 2, no. 6, pp. 691-694, Oct. 2013.
doi: https://doi.org/10.1109/WCL.2013.100913.130660

[3] M. Hsieh and C. Wei, “Channel Estimation for OFDM Systems Based on Comb-Type Pilot Arrangement in Frequency Selective Fading Channels,” *Journal of Consumer Electronics*, vol. 44, no. 1, pp.

217-225, Feb. 1998.
doi: https://doi.org/10.1109/30.663750

[4] 3GPP, "NR: Physical Channels and Modulation, V16.3.0, 3GPP TS 38.211," Sep. 2020.
https://portal.3gpp.org/desktopmodules/Specifications/SpecificationDetails/

[5] ATSC Standard, "Physical Layer Protocol, ATSC A/322," Mar. 2023.
https://www.atsc.org/atsc-documents/type/3-0-standards/

[6] Z. H. Hong, Y. Wu, W. Li and L. Zhang, "High Accuracy Channel Estimation with TxID Sequence in ATSC 3.0 SFN," J*ournal of Broadcast.*, vol. 70, no. 2, pp. 391-400, Jun. 2024.
doi: https://doi.org/10.1109/TBC.2024.3353577

[7] L. Jacobs and M. Moeneclaey, "Effects of MMSE Channel Estimation on BER Performance of Orthogonal Space-Time Block Codes in Rayleigh Fading Channels," *Journal of Communications*, vol. 57, no. 5, pp. 1242-1245, May. 2009.
doi: https://doi.org/10.1109/TCOMM.2009.05.070455

[8] S. Lee, "On the Training of MIMO-OFDM Channels with Least Square Channel Estimation and Linear Interpolation," *Journal of Communications,* vol. 12, no. 2, pp. 100-102, Feb. 2008.
doi: https://doi.org/10.1109/LCOMM.2008.071566

[9] P. Edfors, M. Sandel, J. V. Beek, S. K. Wilson and P. borjesson, "Analysis of DFT-Based Channel Estimation for OFDM," *Journal of Wireless Personal Communications*, vol. 12, no. 1, pp. 55-70, Jan. 2000.
doi: https://doi.org/10.1023/A:1008864109605

[10] Y. Go and J. Kim, "A Study on DFT-Based Channel Estimation for ATSC 3.0 Systems," *Proceeding of International Conference IWAIT,* Jan. 2024, https://www.spiedigitallibrary.org/conference-proceedings-of-spie/13164.toc

[11] K. Yokomakura, S. Sampei, H. Harada and N. Morinaga, "A Carrier Interferometry Based Channel Estimation Technique for MIMO-OFDM/TDMA Systems," *Journal of IEICE Communications,* vol. E90-B, no. 5, pp. 1181-1192, May. 2007.
doi: https://doi.org/10.1093/ietcom/e90-b.5.1181

[12] C. Ahn, "Accurate Channel Identification with Time-Frequency Interferometry for OFDM," *Journal of IEICE Fundamentals*, vol. E90-A, no. 11, pp. 2641-2645, Nov. 2007.
doi: https://doi.org/10.1093/ietfec/e90-a.11.2641

[13] Y. Ida, C. Ahn, T. Masumoto and S. Matsufuji, "Four Time Windows Averaging Channel Estimation with Real and Imaginary TFI Pilot Signals for OFDM," *IEICE Commun. Express*, vol. 6, no. 10, pp.590-595, Oct. 2017.
doi: https://doi.org/10.1587/comex.2017XBL0108

[14] T. Yoshimura, C. Ahn, T. Kamio, H. Fujisaka and K. Haeiwa, "Performance Enhancement of TFI-OFDM with Path Selection Based Channel Identification," *Digital Signal Processing*, vol. 19, no. 5, pp. 852-860, Sep. 2009.
doi: https://doi.org/10.1016/j.dsp.2009.03.008

[15] T. Sakaue, C. Ahn, T. Omori and K. Hasimoto, "Time Domain Replica Signal Based Interference Compensation for SP-MIMO/OFDM with Large Delay Spread Channel," *Journal of Distributed Syst. And Tech*, vol. 5, no. 4, pp. 1-17, Oct. 2014.
doi: https://doi.org/10.4018/ijdst.2014100101

[16] F. Mingming and H. Jin, "An Improved Channel Estimation Algorithm Based on DFT in OFDM System," *Proceeding of International Conference CIBDA*, Apr. 2020.
doi: https://doi.org/10.1109/CIBDA50819.2020.00079

[17] J. Lv, L. Liu, J. Li, H. Yang and Q. Li, "DFT-Based Channel Estimation with Maximum Points Selection for OFDM System," *Proceeding of International Conference ICCSN*, Jun. 2020.
doi: https://doi.org/10.1109/ICCSN52437.2021.9463638

[18] Y. Go and J. Kim, "DFT-Based Channel Estimation using Adaptive Window in ATSC 3.0," *Proceeding of International Conference BMSB,* Jun. 2024.
doi: https://doi.org/10.1109/BMSB62888.2024.10608356

[19] J. A. Kutzner and D. Lung, "Predicting ATSC 3.0 Broadcast Coverage," *Journal of Communications,* vol. 66, no. 10, pp. 281-288, Jan. 2016.
doi: https://doi.org/10.1109/TBC.2015.2505413

[20] H. wu, J. Li, B. Dai and Y. Liu, "Analysis of The Impact of AGC on Cyclic Prefix Length for OFDM Systems," *Journal of Communications, vol.* 66, no. 10, pp. 4783-4794, May. 2018.
doi: https://doi.org/10.1109/TCOMM.2018.2834408

[21] K. Kim, H. Hwang, K. Coi and K. Kim, "Low-Complexity DFT-Based Channel Estimation with Leakage Nulling for OFDM Systems," *Journal of Communications,* vol. 18, no. 3, pp. 415-418, Mar. 2014.
doi: https://doi.org/10.1109/LCOMM.2013.123113.132361

[22] ETSI EN 102.401, "Digital Video Broadcasting (DVB); Transmission to Handheld Terminals (DVB-H); Validation Task Force Report, v.1.1.1," May. 2005, https://www.etsi.org/deliver/etsi_tr/102400_102499/102401/01.01.01_60/tr_102401v010101p.pdf

[23] 3GPP TS 36.101, "Evolved Universal Terrestrial Radio Access (E-UTRA), v.14.3.0," Mar. 2017.
https://portal.3gpp.org/desktopmodules/Specifications/SpecificationDetails.aspx?specificationId=3213

[24] H. Kim, M. Yeom, J. Kim, S. Park, H. Jung and N. Hur, "Performance Evaluation of Channel Estimation Scheme for ATSC 3.0 MIMO under Fixed Reception Environment," *Journal of Broadcasting Eng.*, vol. 24, no. 5, pp. 879-891, Sep. 2019.
doi: https://doi.org/10.5909/JBE.2019.24.5.879

[25] W. Lee, J. Kim, S. Park and N. Hur, "Study on 22 MIMO Detection in ATSC 3.0 Systems," *Journal of Broadcasting Eng.,* vol. 22, no. 6, pp. 755-764, Nov. 2017.
doi: https://doi.org/10.5909/JBE.2017.22.6.755

[26] J. Kim, H. Kim, S. Park and H. Kim, "Study on Synchronization Using Bootstrap Signals for ATSC 3.0 Systems," *Journal of Broadcasting Eng*., vol. 21, no. 6, pp. 899-912, Nov. 2016.
doi: https://doi.org/10.5909/JBE.2016.21.6.899

[27] S. Ahn, S. Park, J. Lee, B. Lim, S. Kwon, N. Hur, Y. Wu, L. Zhang, W. Li and J. Kim "Mobile Performance Evaluation for ATSC 3.0 Physical Layer Modulation and Code Combinations Under TU-6 Channel," *Journal of Broadcast.,* vol. 66, no. 4, pp. 752-769, Dec. 2020.
doi: https://doi.org/10.1109/TBC.2019.2954065

[28] S. Kwon, S. Ahn, S. Ahn, S. Jeon, S. Shima, M. Aitken, A. Saha, P. M. Maru, P. Naik and S. Park, “Comparative Assessment of Physical Layer Performance: ATSC 3.0 vs. 5G Broadcast in Laboratory and Field Tests,” *Journal of Broadcast*., vol. 71, no. 1, pp. 2-10, March. 2025.
doi: https://doi.org/10.1109/TBC.2024.3482183

[29] S. Ahn, J. Kim, S. Ahn, S. Kwon, S. Jeon and D. Gomez-Barquero, P. Angueira, D. He, C. Akamine, M. Ek, S. Simha, M. Aitken, Z. H. Hong, Y. Wu and S. Park, “Characterization and Modeling of UHF Wireless Channel in Terrestrial SFN Environments: Urban Fading Profiles,” *Journal of Broadcast.*, vol. 68, no. 4, pp. 803-818, Dec. 2022.
doi: https://doi.org10.1109/TBC.2022.3210382

저 자 소 개

고 영 빈

- 2023년 8월 : 한국해양대학교 전자전기정보공학부 (공학사)
- 2025년 2월 : 한국해양대학교 전자통신공학과 (공학석사)
- ORCID : https://orcid.org/0009-0005-8922-5920
- 주관심분야 : 디지털방송시스템, 이동통신시스템, 디지털신호처리

김 정 창

- 2000년 2월 : 한양대학교 전자·전자통신·전파공학과군(공학사)
- 2002년 2월 : 포항공과대학교 전자컴퓨터공학부(공학석사)
- 2006년 8월 : 포항공과대학교 전자컴퓨터공학부(공학박사)
- 2006년 9월 ~ 2008년 5월 : 포항공과대학교 정보통신연구소 전임연구원
- 2008년 5월 ~ 2009년 8월 : 포항공과대학교 미래정보기술사업단 연구조교수
- 2009년 8월 ~ 2010년 8월 : 한국전자통신연구원 선임연구원
- 2010년 9월 ~ 현재 : 한국해양대학교 전자전기정보공학부 교수
- 2017년 ~ 현재 : ETRI Journal, 편집위원
- 2018년 ~ 현재 : IEEE Transactions on Broadcasting, Associate Editor
- ORCID : https://orcid.org/0000-0002-8612-9360
- 주관심분야 : 무선통신시스템, 디지털방송 전송시스템, 5G/6G